

Chainlike Mesoporous SnO₂ as a Well-Performing Catalyst for Electrochemical CO₂ Reduction

Original

Chainlike Mesoporous SnO₂ as a Well-Performing Catalyst for Electrochemical CO₂ Reduction / Bejtka, Katarzyna; Zeng, Juqin; Sacco, Adriano; Castellino, Micaela; Hernández, Simelys; Farkhondeh, M. Amin; Savino, Umberto; Ansaloni, Simone; Pirri, Candido F.; Chiodoni, Angelica. - In: ACS APPLIED ENERGY MATERIALS. - ISSN 2574-0962. - ELETTRONICO. - 2:5(2019), pp. 3081-3091. [10.1021/acsaem.8b02048]

Availability:

This version is available at: 11583/2734428 since: 2020-01-14T10:27:19Z

Publisher:

American Chemical Society

Published

DOI:10.1021/acsaem.8b02048

Terms of use:

openAccess

This article is made available under terms and conditions as specified in the corresponding bibliographic description in the repository

Publisher copyright

(Article begins on next page)

Supporting Information

Chainlike Mesoporous SnO₂ as a Well-Performing Catalyst for Electrochemical CO₂ Reduction

Katarzyna Bejtka^{,†}, Juqin Zeng^{*,†}, Adriano Sacco[†], Micaela Castellino[‡], Simelys Hernández[†],
M. Amin Farkhondehfal[†], Umberto Savino^{†,‡}, Simone Ansaloni[‡], Candido F. Pirri^{†,‡} and
Angelica Chiodoni[†]*

[†] Center for Sustainable Future Technologies @POLITO, Istituto Italiano di Tecnologia, Via Livorno 60, 10144 Turin, Italy

[‡] Department of Applied Science and Technology, Politecnico di Torino, Corso Duca degli Abruzzi 24, 10129 Turin, Italy

*E-mail: Katarzyna.Bejtka@iit.it, *E-mail: Juqin.Zeng@iit.it

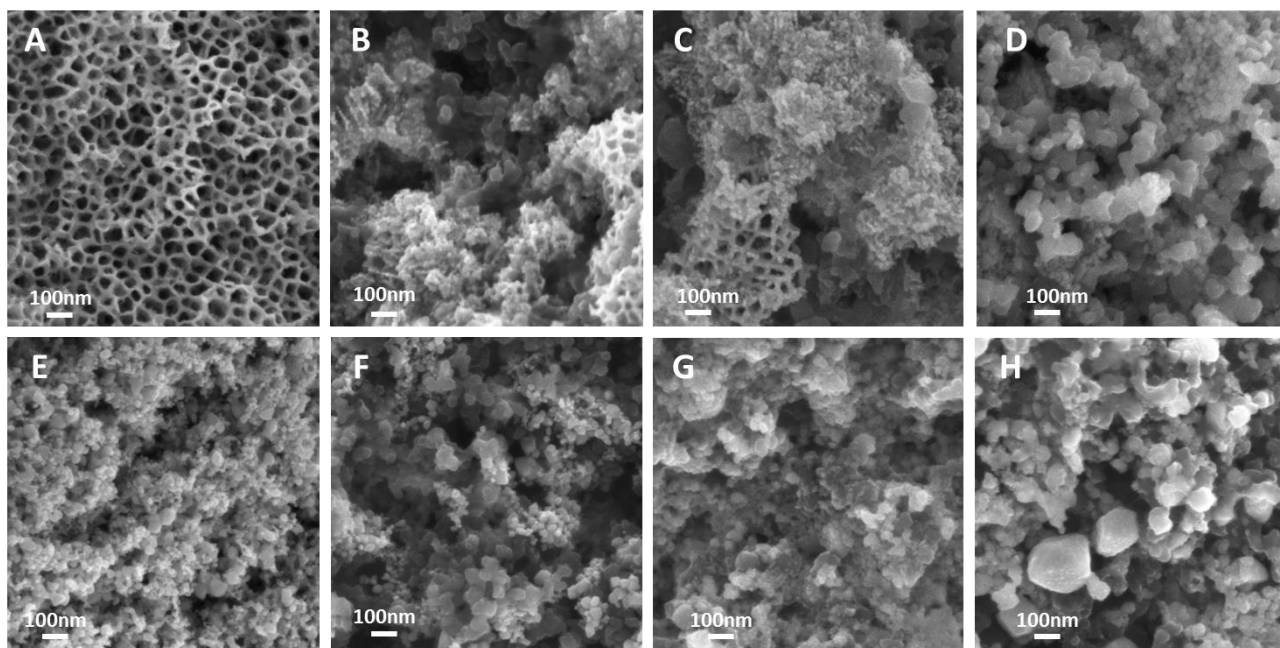


Figure S1 Top view FESEM images of the (a) as-grown SnO_2 , (b) as-prepared electrode SnO_2 -anod, (c) SnO_2 -anod electrode reduced for 20min and (d) tested SnO_2 -anod electrode, (e) commercial SnO_2 , (f) as-prepared electrode SnO_2 -comm, (g) SnO_2 -comm electrode reduced for 20min and (h) tested SnO_2 -comm electrode. All images are shown at the same magnification.

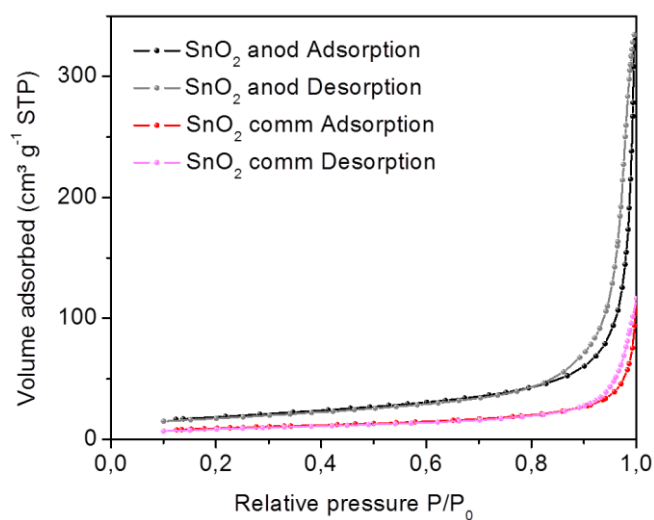


Figure S2 N_2 adsorption/desorption isotherms for SnO_2 prepared via anodic oxidation and commercial.

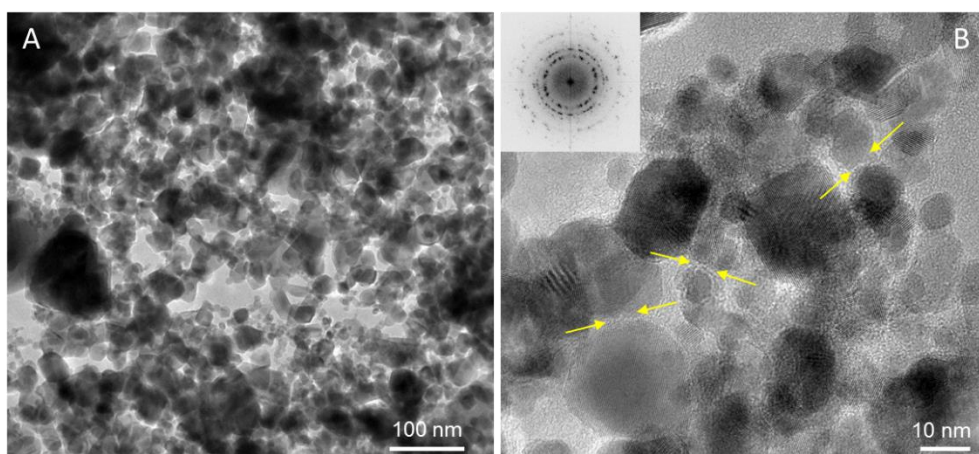


Figure S3 TEM image at two different magnification of the commercial SnO_2 . In the inset the FFT of picture (b) is also reported.

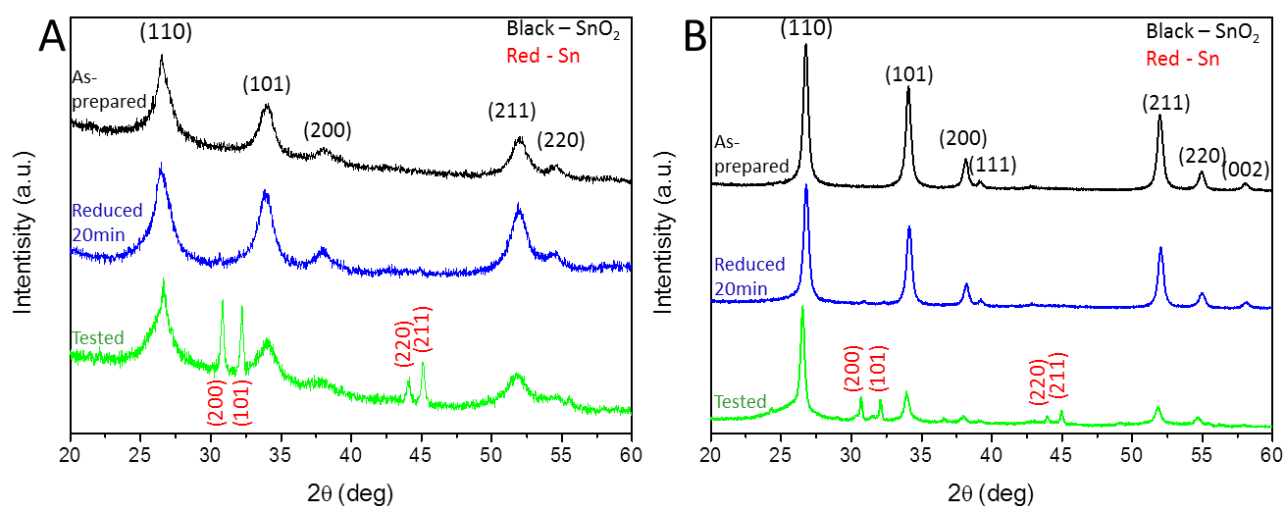


Figure S4 XRD patterns of (a) SnO_2 -anod and (b) SnO_2 -comm electrodes (as-prepared, reduced for 20min and tested).

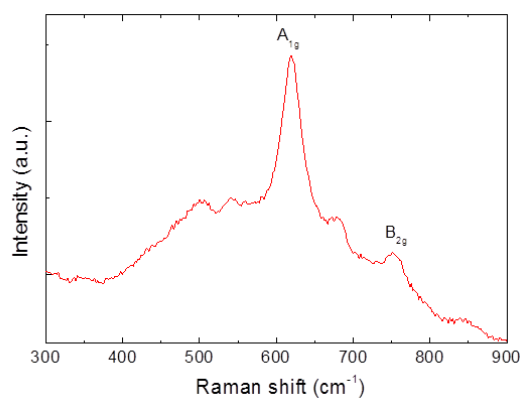


Figure S5 Raman spectrum of as-prepared SnO_2 -anod electrode.

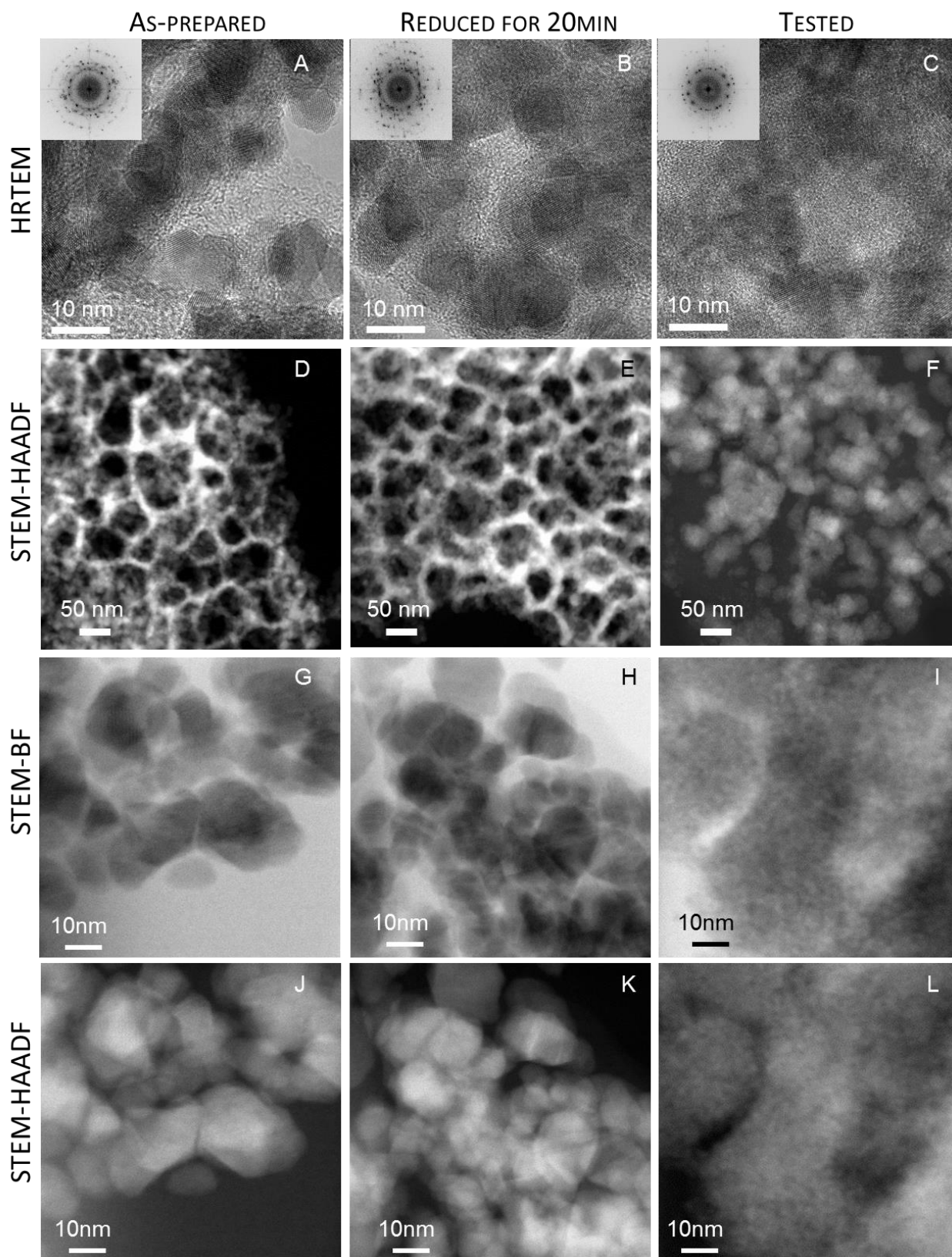


Figure S6 TEM study of the crystals evolution of the SnO₂-anod, including the as-prepared, reduced for 20 minutes and long term tested material. In the rows the following images are shown: HRTEM with FFT (of the shown area) in the inset, low magnification HAADF-STEM image, high magnification BF-STEM and HAADF-STEM.

The double-layer capacitance (C_{dl}) values of the SnO_2 -comm, SnO_2 -anod and Sn foil electrodes are evaluated by cyclic voltammetry (CV) at various scan rates in a potential range between -0.29 V and -0.39 V. The geometric current densities are plotted against the scan rates, and the slope of the linear fitting quantifies the double-layer capacitance C_{dl} .

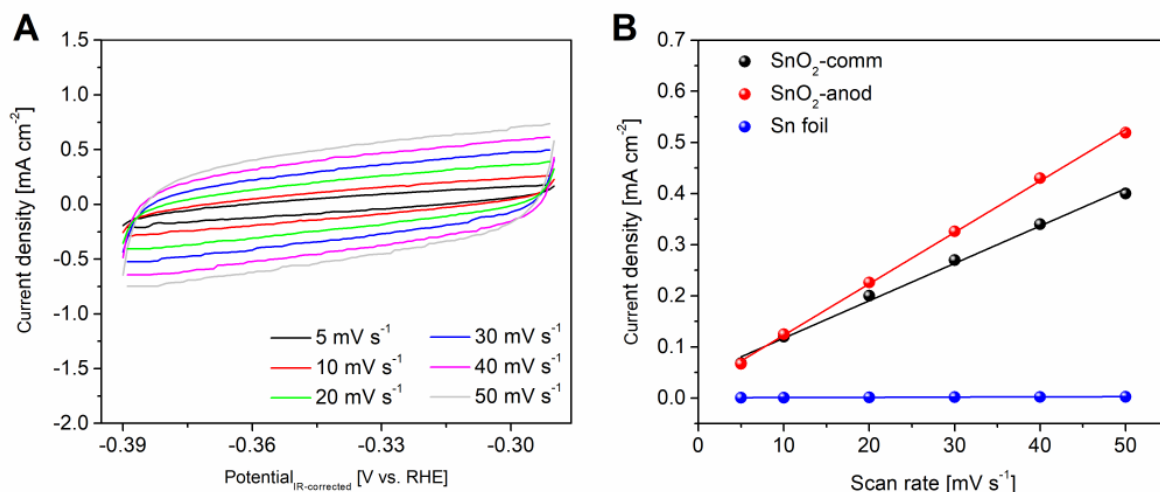


Figure S7 Determination of double-layer capacitance for various electrodes in CO_2 -saturated 0.1 M KHCO_3 : (a) representing CVs on SnO_2 -anod electrode; (b) Capacitance values calculated from the slopes of current densities vs. scan rate.

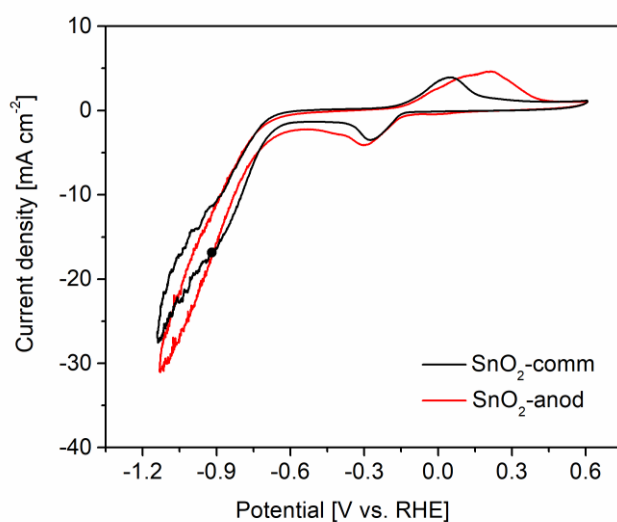


Figure S8 Comparison of the voltammograms of SnO_2 -comm and SnO_2 -anod in the CO_2 -saturated electrolyte.

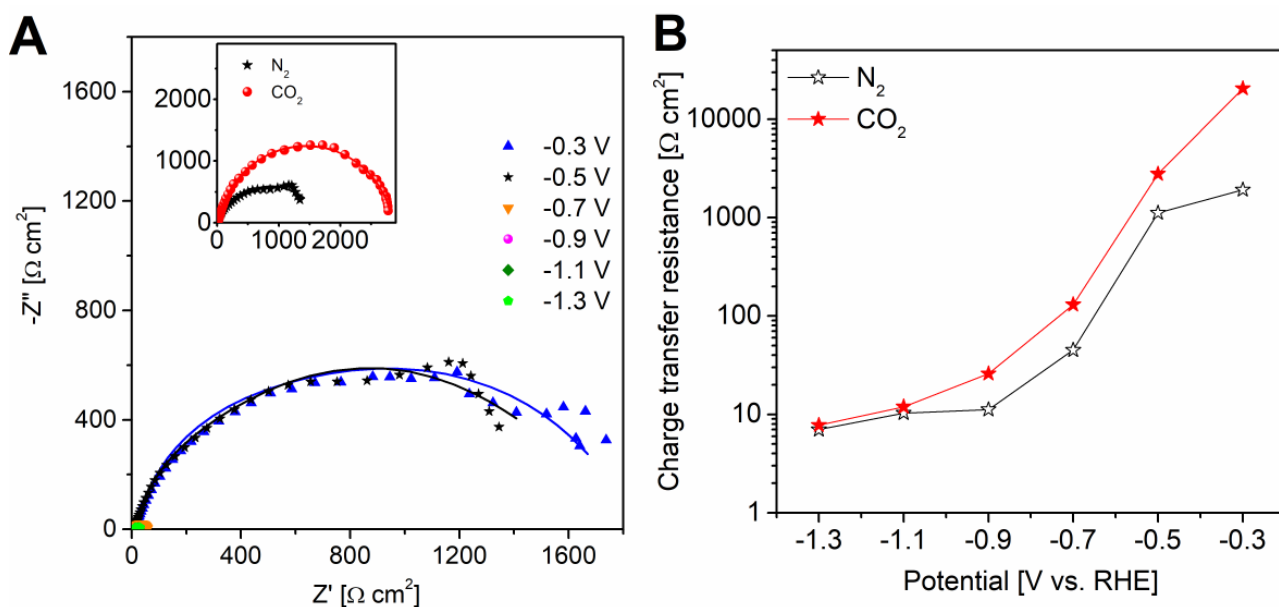


Figure S9 EIS analysis on a Sn foil electrode: (a) Nyquist plots obtained in N_2 -saturated electrolyte (the points are experimental data, the clines are the curves calculated through fitting. In the inset, the two spectra acquired at -0.5 V in N_2 - and CO_2 -saturated solutions are shown. (b) Charge transfer resistances reported as a function of the potential.

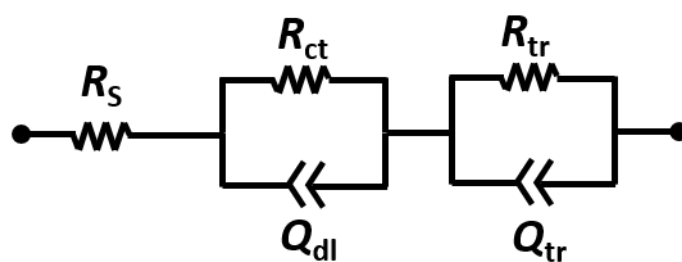


Figure S10 Equivalent circuit used for fitting of EIS data.

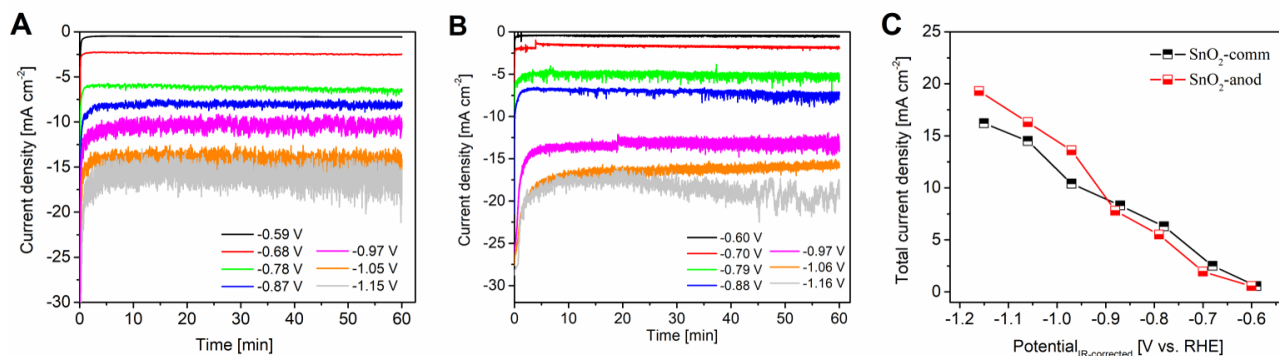


Figure S11 CA measurements carried out in CO₂-saturated 0.1 M KHCO₃ aqueous solution at different potentials: (a) SnO₂-comm; (b) SnO₂-anod; (c) Comparison of total current densities on SnO₂-comm and SnO₂-anod electrodes at various potentials.

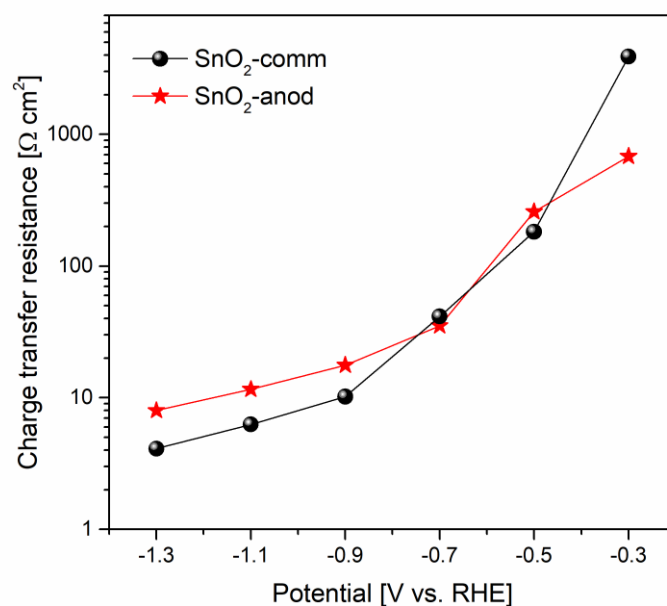


Figure S12 Comparison of charge transfer resistance obtained from EIS on SnO₂-comm and SnO₂-anod electrodes at various potentials.

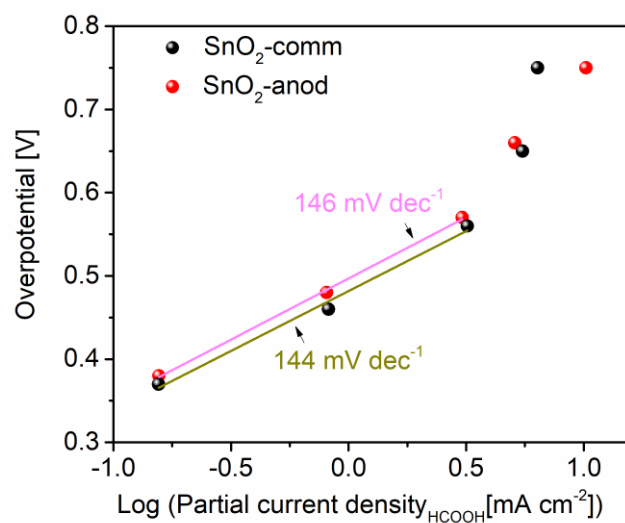


Figure S13 Tafel plot analysis for HCOOH production on SnO₂-comm and SnO₂-anod electrodes.

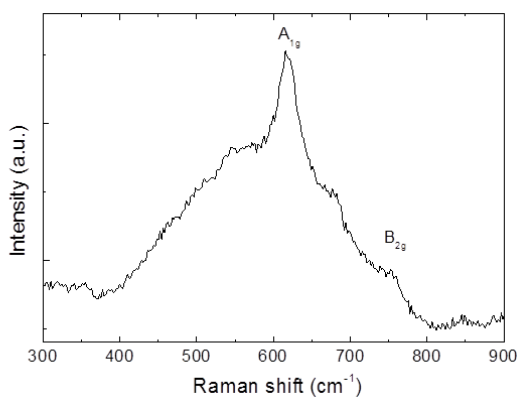


Figure S14 Raman spectrum of tested SnO₂-anod electrode.

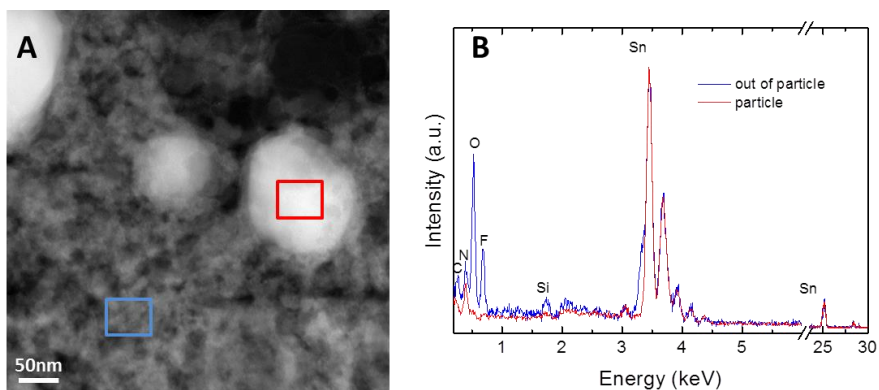


Figure S15 STEM image of the cross-section lamella of tested SnO₂-anod electrode (a) and EDX measurement performed locally in the particle and out of the particle (b).

Table S1 Comparison of electrocatalytic performance for reducing CO₂ to formic acid / formate on tin-based catalysts.

Electrode	Electrolyte	Maximum Faradic Efficiency [%]	Total current (mA cm ⁻²)	Ref
Sn/SnO ₂ porous hollow fiber	0.1 M KHCO ₃	82% @ -1.6 V (vs. SCE)	28,6	1
SnO ₂ nanosheets/Carbon cloth	0.5 M NaHCO ₃	87% @ -1.6 V (vs. Ag/AgCl)	48,6	2
SnO _x NPs	0.5 M KHCO ₃	87% @ -1.6 V (vs. SHE)	14,0	3
Electro deposited Sn	0.1 M KHCO ₃	91% @ -1.4 V (vs. SCE)	15,0	4
Sn particles	0.5 M KHCO ₃	73% @ -1.8 V (vs. Ag/AgCl)	13,5	5
SnO ₂ nanopowder	0.5 M NaOH	68% @ -0.6 V (vs. RHE)	3,5	6
SnO ₂ /graphene	0.1 M NaHCO ₃	94% @ -1.8 V (vs. SCE)	10,2	7
SnO ₂ /carbon black	0.1 M NaHCO ₃	86% @ -1.8 V (vs. SCE)	5,4	7
Sn dendrite	0.1 M KHCO ₃	72% @ -1.36 V (vs. RHE)	17,1	8
Sn - Nafion	0.5 M NaHCO ₃	70% @ -1.6 V (vs. NHE)	27,0	9
SnO ₂ /carbon aerogel	1.0 M KHCO ₃	76% @ -0.96 V (vs. RHE)	23,5*	10
SnO ₂ Porous NWs	0.1 M KHCO ₃	80% @ -0.8 V (vs. RHE)	6,0	11
SnO ₂ NPs	0.1 M KHCO ₃	58% @ -0.8 V (vs. RHE)	2,4	11
SnO ₂ at N-rGO	0.5 M NaHCO ₃	78% @ -0.8 V (vs. RHE)	21,3	12
SnO ₂ nanospheres	0.5 M KHCO ₃	56% @ -1.1 V (vs. RHE)	6,0*	13
Mesoporous SnO ₂	0.1 M KHCO ₃	40% @ -0.8 V (vs. RHE)	5.0	14
		40% @ -1.4 V (vs. RHE)	21.3	14
Chain-like mesoporous SnO ₂	0.1 M KHCO ₃	82% @ -1.06 V (vs. RHE)	16,3	This work
		80% @ -1.15 V (vs. RHE)	19.3	This work
SnO ₂ nanopowder	0.1 M KHCO ₃	43% @ -1.15 V (vs. RHE)	16.2	This work
		67% @ -0.87 V (vs. RHE)	8.3	This work

* estimated on the basis of information given in the paper

References

- (1) Hu H., Gui L., Zhou W., Sun J., Xu J., Wang Q., He B., Zhao L. Partially reduced Sn/SnO₂ porous hollow fiber: A highly selective, efficient and robust electrocatalyst towards carbon dioxide reduction. *Electrochimica Acta* **2018**, 285, 70-77.
- (2) Li F., Chen L., Knowles G.P., MacFarlane D.R., Zhang J. Hierarchical Mesoporous SnO₂ Nanosheets on Carbon Cloth: A Robust and Flexible Electrocatalyst for CO₂ Reduction with High Efficiency and Selectivity, *Angew. Chem. Int. Ed.* **2017**, 56, 505-509.
- (3) Li Y., Qiao J., Zhang X., Lei T., Girma A., Liu Y., Zhang J. Rational Design and Synthesis of SnO_x Electrocatalysts with Coralline Structure for Highly Improved Aqueous CO₂ Reduction to Formate. *ChemElectroChem* **2016**, 3, 1618 – 1628.
- (4) Zhao C.C., Wang J.L. Electrochemical reduction of CO₂ to formate in aqueous solution using electro-deposited Sn catalysts. *Chem. Eng. J.* **2016**, 293, 161–170.
- (5) Wang Q., Dong H., Yu H. Fabrication of a novel tin gas diffusion electrode for electrochemical reduction of carbon dioxide to formic acid. *RSC Adv.* **2014**, 4, 59970–59976.
- (6) Lee S., Ocon J.D., Son Y., Lee J. Alkaline CO₂ Electrolysis toward Selective and Continuous HCOO⁻ Production over SnO₂ Nanocatalysts. *J. Phys. Chem. C* **2015**, 119, 4884–4890.
- (7) Zhang, S., Kang, P., Meyer, T.J. Nanostructured Tin Catalysts for Selective Electrochemical Reduction of Carbon Dioxide to Formate. *J. Am. Chem. Soc.* **2014**, 136, 1734–1737.
- (8) Won D.H., Choi C.H., Chung J.H., Chung M.W., Kim E.H., Woo S.I. Rational Design of a Hierarchical Tin Dendrite Electrode for Efficient Electrochemical Reduction of CO₂. *ChemSusChem* **2015**, 8, 3092–3098.
- (9) Surya Prakash G.K., Viva F.A., Olah G.A. Electrochemical reduction of CO₂ over Sn-Nafion coated electrode for a fuel-cell-like device. *J. Power Sources* **2012**, 223, 68–73.
- (10) Yu J., Liu H., Song S., Wang Y., Tsiakaras P. Electrochemical reduction of carbon dioxide at nanostructured SnO₂/carbon aerogels: The effect of tin oxide content on the catalytic activity and formate selectivity. *Appl. Catal. A, General* **2017**, 545, 159–166.
- (11) Kumar B., Atla V., Brian J.P., Kumari S., Nguyen T.Q., Sunkara M., Spurgeon J.M. Reduced SnO₂ Porous Nanowires with a High Density of Grain Boundaries as Catalysts for Efficient Electrochemical CO₂-into-HCOOH Conversion. *Angew. Chem. Int. Ed.* **2017**, 56, 3645–3649.
- (12) Zhang B., Guo Z., Zuo Z., Pan W., Zhang J. The Ensemble Effect of Nitrogen Doping and Ultrasmall SnO₂ Nanocrystals on Graphene Sheets for Efficient Electroreduction of Carbon Dioxide. *Appl. Catal. B. Environ.* **2018**, 239, 441–449.

- (13) Fu Y., Li Y., Zhang X., liu Y., Zhou X., Qiao J. Electrochemical CO₂ reduction to formic acid on crystalline SnO₂ nanosphere catalyst with high selectivity and stability. *Chinese Journal of Catalysis* **2016**, 37, 1081–1088.
- (14) Ge H., Gu Z., Han P., Shen H., Al-Enizi A. M., Zhang L., Zheng G. J. Mesoporous Tin Oxide for Electrocatalytic CO₂ Reduction. *Colloid Interface Sci.* **2018**, 531, 564-569.